Since January 2020 Elsevier has created a COVID-19 resource centre with free information in English and Mandarin on the novel coronavirus COVID-19. The COVID-19 resource centre is hosted on Elsevier Connect, the company's public news and information website.

Comparative tropism, replication kinetics, and cell damage profiling of SARS-CoV-2 and SARS-CoV with implications for clinical manifestations, transmissibility, and laboratory studies of COVID-19: an observational study

Hin Chu, Jasper Fuk-Woo Chan*, Terrence Tsz-Tai Yuen*, Huiping Shuai*, Shuofeng Yuan, Yixin Wang, Bingjie Hu, Cyril Chik-Yan Yip, Jessica Oi-Ling Tsang, Xiner Huang, Yue Chai, Dong Yang, Yuxin Hou, Kenn Ka-Heng Chik, Xi Zhang, Agnes Yim-Fong Fung, Hoi-Wah Tsoi, Jian-Piao Cai, Wan-Mui Chan, Jonathan Daniel Ip, Allen Wing-Ho Chu, Jie Zhou, David Christopher Lung, Kin-Hang Kok, Kelvin Kai-Wang To, Owen Tak-Yin Tsang, Kwok-Hung Chan, Kwok-Yung Yuen*

Summary

Background Severe acute respiratory syndrome coronavirus 2 (SARS-CoV-2) was reported from China in January, 2020. SARS-CoV-2 is efficiently transmitted from person to person and, in 2 months, has caused more than 82 000 laboratory-confirmed cases of coronavirus disease 2019 (COVID-19) and 2800 deaths in 46 countries. The total number of cases and deaths has surpassed that of the 2003 severe acute respiratory syndrome coronavirus (SARS-CoV). Although both COVID-19 and severe acute respiratory syndrome (SARS) manifest as pneumonia, COVID-19 is associated with apparently more efficient transmission, fewer cases of diarrhoea, increased mental confusion, and a lower crude fatality rate. However, the underlying virus–host interactive characteristics conferring these observations on transmissibility and clinical manifestations of COVID-19 remain unknown.

Methods We systematically investigated the cellular susceptibility, species tropism, replication kinetics, and cell damage of SARS-CoV-2 and compared findings with those for SARS-CoV. We compared SARS-CoV-2 and SARS-CoV replication in different cell lines with one-way ANOVA. For the area under the curve comparison between SARS-CoV-2 and SARS-CoV replication in Calu3 (pulmonary) and Caco2 (intestinal) cells, we used Student's *t* test. We analysed cell damage induced by SARS-CoV-2 and SARS-CoV with one-way ANOVA.

Findings SARS-CoV-2 infected and replicated to comparable levels in human Caco2 cells and Calu3 cells over a period of 120 h (p=0·52). By contrast, SARS-CoV infected and replicated more efficiently in Caco2 cells than in Calu3 cells under the same multiplicity of infection (p=0·0098). SARS-CoV-2, but not SARS-CoV, replicated modestly in U251 (neuronal) cells (p=0·036). For animal species cell tropism, both SARS-CoV and SARS-CoV-2 replicated in non-human primate, cat, rabbit, and pig cells. SARS-CoV, but not SARS-CoV-2, infected and replicated in *Rhinolophus sinicus* bat kidney cells. SARS-CoV-2 consistently induced significantly delayed and milder levels of cell damage than did SARS-CoV in non-human primate cells (VeroE6, p=0·016; FRhK4, p=0·0004).

Interpretation As far as we know, our study presents the first quantitative data for tropism, replication kinetics, and cell damage of SARS-CoV-2. These data provide novel insights into the lower incidence of diarrhoea, decreased disease severity, and reduced mortality in patients with COVID-19, with respect to the pathogenesis and high transmissibility of SARS-CoV-2 compared with SARS-CoV.

Funding May Tam Mak Mei Yin, The Shaw Foundation Hong Kong, Richard Yu and Carol Yu, Michael Seak-Kan Tong, Respiratory Viral Research Foundation, Hui Ming, Hui Hoy and Chow Sin Lan Charity Fund, Chan Yin Chuen Memorial Charitable Foundation, Marina Man-Wai Lee, The Hong Kong Hainan Commercial Association South China Microbiology Research Fund, The Jessie & George Ho Charitable Foundation, Perfect Shape Medical, The Consultancy Service for Enhancing Laboratory Surveillance of Emerging Infectious Diseases and Research Capability on Antimicrobial Resistance for the Department of Health of the Hong Kong Special Administrative Region Government, The Theme-Based Research Scheme of the Research Grants Council, Sanming Project of Medicine in Shenzhen, and The High Level-Hospital Program, Health Commission of Guangdong Province, China.

Lancet Microbe 2020

Published Online
April 21, 2020
https://doi.org/10.1016/S2666-5247(20)30004-5

See Online/Comment
https://doi.org/10.1016/S2666-5247(20)30008-2

*Joint first authors

State Key Laboratory of Emerging Infectious Diseases, Carol Yu Centre for Infection, Department of Microbiology, Li Ka Shing Faculty of Medicine, The University of Hong Kong, Pokfulam, Hong Kong Special Administrative Region, China (H Chu PhD, J F-W Chan MD, T T-T Yuen BA, H Shuai PhD, S Yuan PhD, Y Wang MPhil, B Hu MPhil, C C-Y Yip PhD, J O-L Tsang BSc, X Huang BSc, Y Chai MPhil, D Yang MPhil, Y Hou MPhil, K K-H Chik MMedSc, X Zhang BSc, A Y-F Fung BSc, H-W Tsoi MPhil, J-P Cai BSc, W-M Chan PhD, J D Ip MSc, A W-H Chu MSc, J Zhou PhD, K-H Kok PhD, K K-W To MD, K-H Chan PhD); **Department of Pathology, Queen Elizabeth Hospital, Hong Kong Special Administrative Region, China** (D C Lung FRCPath); **Department of Medicine and Geriatrics, Princess Margaret Hospital, Hong Kong Special Administrative Region, China** (O T-Y Tsang FRCP); **and Department of Clinical Microbiology and Infection Control, The University of Hong Kong-Shenzhen Hospital, Shenzhen, China** (J F-W Chan, K K-W To, Prof K-Y Yuen MD)

Introduction

Coronaviruses are enveloped, positive-sense, single-stranded RNA viruses that can infect a wide range of human and animal species. Before December, 2019, six human pathogenic coronaviruses were known. Severe acute respiratory syndrome coronavirus

Correspondence to:
Prof Kwok-Yung Yuen,
Department of Clinical Microbiology and Infection Control, The University of Hong Kong-Shenzhen Hospital, Shenzhen 518009, China
kyyuen@hku.hk

Research in context

Evidence before this study

We searched PubMed on Feb 28, 2020, with the terms "SARS-CoV-2", "2019-nCoV", or "novel coronavirus" and "susceptibility", "tropism", "replication", or "cell damage". We had no start date limitations but did restrict our search to articles published in English. Our search did not identify any original research article that investigated the susceptibility, tropism, replication, or cytotoxicity of severe acute respiratory syndrome coronavirus 2 (SARS-CoV-2).

Added value of this study

We investigated cell susceptibility, species tropism, replication kinetics, and virus-induced cell damage of SARS-CoV-2 and severe acute respiratory syndrome coronavirus (SARS-CoV) using live infectious virus particles. SARS-CoV-2 replicated more efficiently than did SARS-CoV in human pulmonary (Calu3) cells. By contrast, SARS-CoV (but not SARS-CoV-2) replicated efficiently in *Rhinolophus sinicus* bat kidney cells. Moreover, SARS-CoV-2 was consistently found to induce less cell damage than SARS-CoV in non-human primate kidney (VeroE6) cells. These findings provide a possible explanation for the efficient person-to-person transmission of coronavirus disease 2019 (COVID-19), because SARS-CoV-2 has most likely adapted well to humans and, thus, is no longer able to propagate well in bat cells, and SARS-CoV-2 can replicate to high levels without inducing substantial host cell damage. Furthermore, SARS-CoV-2 replicated similarly efficiently in human intestinal (Caco2) and pulmonary cells, but SARS-CoV replicated significantly better in intestinal than pulmonary cells. This difference might account for why diarrhoea has been reported much less frequently in patients with COVID-19 than in those infected with SARS-CoV. SARS-CoV-2 (but not SARS-CoV) also modestly replicated in neuronal (U251) cells, highlighting the potential that this virus can cause neurological manifestations (eg, confusion, anosmia, and ageusia) in patients with COVID-19. Finally, SARS-CoV-2 replicated efficiently in non-human primate, cat, rabbit, and pig cells. These results would be useful for development of COVID-19 animal models.

Implications of all the available evidence

Our findings provide explanations at the tissue cell culture level for differences in clinical manifestations and transmissibility between SARS-CoV-2 and SARS-CoV. Our data will be useful for optimising animal models and laboratory methods for COVID-19.

(SARS-CoV) and Middle East respiratory syndrome coronavirus (MERS-CoV) can cause severe acute atypical pneumonia with extrapulmonary manifestations in both immunocompetent and immunocompromised patients. Human coronavirus 229E (HCoV-229E), HCoV-NL63, HCoV-OC43, and HCoV-HKU1 usually cause mild and self-limiting upper respiratory tract infections in immunocompetent patients and, occasionally, lower respiratory tract infections in immunocompromised hosts.[1] On Dec 31, 2019, WHO was informed of a cluster of unexplained cases of pneumonia in Wuhan, Hubei province, China. Subsequent investigations identified a novel lineage B betacoronavirus (later named severe acute respiratory syndrome coronavirus 2 [SARS-CoV-2]) with a high degree of genomic similarity with bat coronaviruses.[2–4]

The typical clinical features of SARS-CoV-2 infection, or coronavirus disease 2019 (COVID-19), are similar to severe acute respiratory syndrome (SARS) and include fever, myalgia, dry cough, dyspnoea, fatigue, and radiological evidence of ground-glass lung opacities compatible with atypical pneumonia.[5–7] However, important clinical differences between COVID-19 and SARS have been increasingly recognised. For example, diarrhoea is seen much less frequently in patients with COVID-19 (2·0–10·1%) than in those with SARS (20·1%).[5–9] Neurological manifestations such as confusion are infrequently reported in patients with COVID-19 (9·1%) but are almost absent in patients with SARS.[8]

Another apparent difference between SARS-CoV-2 and SARS-CoV is the speed at which the COVID-19 outbreak is expanding. Within just 2 months, the number of laboratory-confirmed COVID-19 cases worldwide has already exceeded the total number of SARS cases by nearly ten times. The mean basic reproduction number (R_0) of COVID-19 has been estimated to be similar to that of SARS (roughly 3·0).[10,11] However, in the epicentre of outbreak in Hubei province, the R_0 of COVID-19 could be as high as 6·49.[12] Although the COVID-19 pandemic might be related to various geographical and social factors, such as the high population density in Wuhan, the massive population movement before the Spring Festival, and control measures implemented by health authorities during the different phases of the outbreak, it remains unclear whether SARS-CoV-2 possesses viral factors that are associated with higher transmissibility than SARS-CoV.

As shown by SARS-CoV, MERS-CoV, and other emerging viruses, cell culture models are useful for characterising cell tropism, viral replication kinetics, and virus-induced cell damage profiles of novel viruses.[13–15] To date, these important biological characteristics of infectious SARS-CoV-2 in tissue cell cultures remain incompletely understood. In this study, we analysed the differential susceptibilities of 25 cell lines derived from different human organ tissues and non-human animal species and compared findings in SARS-CoV-2 and SARS-CoV. Our findings could provide potential explanations at tissue culture level for noted differences in clinical manifestations and transmission characteristics between SARS-CoV-2 and SARS-CoV, as well as information for the rational design of diagnostics and research methods for COVID-19.

Panel: Primers and probes

Forward primer for both SARS-CoV-2 and SARS-CoV
5′-CGCATACAGTCTTRCAGGCT-3′

Reverse primer for both SARS-CoV-2 and SARS-CoV
5′-GTGTGATGTTGAWATGACATGGTC-3′

SARS-CoV-2-specific probe
5′-FAM-TTAAGATGTGGTGCTTGCATACGTAGAC-IABkFQ-3′

SARS-CoV-specific probe
5′-Cy5-CTTCGTTGCGGTGCCTGTATTAGG-IAbRQSp-3′

SARS-CoV-2=severe acute respiratory syndrome coronavirus 2. SARS-CoV=severe acute respiratory syndrome coronavirus.

Methods

Viruses and biosafety

We isolated SARS-CoV-2 HKU-001a from a nasopharyngeal aspirate specimen taken from a patient from Hong Kong with laboratory-confirmed COVID-19. We inoculated the nasopharyngeal aspirate specimen on VeroE6 (non-human primate kidney) cells, with and without 0·5 µg/mL trypsin. We monitored the inoculated cells daily for cytopathic effects by light microscopy, and we collected cell supernatant daily for quantitative RT-PCR to assess the viral load. Substantial cytopathic effects were seen at 72 h postinoculation (hpi), and we confirmed positive SARS-CoV-2 replication by quantitative RT-PCR using specific primers and probes against SARS-CoV-2 (panel).[16] We did whole-genome sequencing of the SARS-CoV-2 isolate using an Oxford Nanopore MinION device (Oxford Nanopore Technologies, Oxford, UK) supplemented by Sanger sequencing, as previously described.[4] Sequence comparisons between SARS-CoV-2 HKU-001a and clinical isolates are shown in the appendix (pp 1–2). SARS-CoV was a clinical isolate archived at the Department of Microbiology, The University of Hong Kong. Both SARS-CoV-2 HKU-001a (GenBank accession number MT230904) and SARS-CoV GZ50 (AY304495) were propagated and the titre ascertained in VeroE6 cells with plaque assays. Both viruses were passaged three times before being used for experiments. All experiments entailing live SARS-CoV-2 and SARS-CoV followed the approved standard operating procedures of our biosafety level 3 facility.[13,17]

Phylogenetic analysis of SARS-CoV-2 and SARS-CoV

Three nucleotide sequences of SARS-CoV-2 (GenBank accession numbers MN938384, MN975262, and MT230904) and two nucleotide sequences of SARS-CoV (AY278491 and AY304495) were first aligned using MUSCLE.[18] We used aligned sequences for the determination of best model and for the phylogenetic analysis using MEGA X.[19]

	Abbreviation	Source of cell line
Human respiratory tract		
Lung adenocarcinoma	A549	ATCC CCL-185
Lung adenocarcinoma	Calu3	ATCC HTB-55
Embryonic lung fibroblasts	HFL	In-house development
Human gastrointestinal tract		
Colorectal adenocarcinoma	Caco2	ATCC HTB-37
Human liver		
Hepatocellular carcinoma	Huh7	JCRB0403, JCRB cell bank of Okayama University
Human cervix		
Cervical adenocarcinoma	HeLa	ATCC CCL-2
Human kidney		
Embryonic kidney	293T	ATCC CRL-3216
Human neuronal		
Glioblastoma	U251	Sigma 09063001 (Sigma-Aldrich, St Louis, MO, USA)
Human muscle		
Rhabdomyosarcoma	RD	ATCC CCL-136
Bat		
Rousettus leschenaultii lung	RLL	In-house development
Rousettus leschenaultii kidney	RLK	In-house development
Rhinolophus sinicus lung	RSL	In-house development
Rhinolophus sinicus kidney	RSK	In-house development
Porcupine		
Porcupine kidney	PoK	In-house development
Non-human primate		
African green monkey kidney (clone of Vero-76)	VeroE6	ATCC CRL-1586
Rhesus monkey kidney	FRhK4	ATCC CRL-1688
Rhesus monkey kidney	LLCMK2	ATCC CCL-7
Dog		
Madin-Darby canine kidney	MDCK	ATCC CCL-34
Cat		
Feline kidney	CRFK	ATCC CCL-94
Pig		
Porcine kidney	PK-15	ATCC CCL-33
Rabbit		
Rabbit kidney	RK-13	ATCC CCL-37
Chicken		
Chicken fibroblasts	DF-1	ATCC CRL-12203
Mouse		
Murine fibroblast	L929	ATCC CCL-1
Murine embryonic fibroblast	3T3	ATCC CRL-1658
Hamster		
Hamster kidney fibroblast	BHK21	ATCC CCL-10

ATCC=American Type Culture Collection (Manassas, VA, USA). JCRB=Japanese Collection of Research Bioresources (National Institutes of Biomedical Innovation, Health and Nutrition, Osaka, Japan).

Table: **Human and non-human cell lines used in the study**

Cell culture and virus infection

We inoculated 25 cell lines derived from different tissues or organs and host species (table) with SARS-CoV-2 or

See Online for appendix

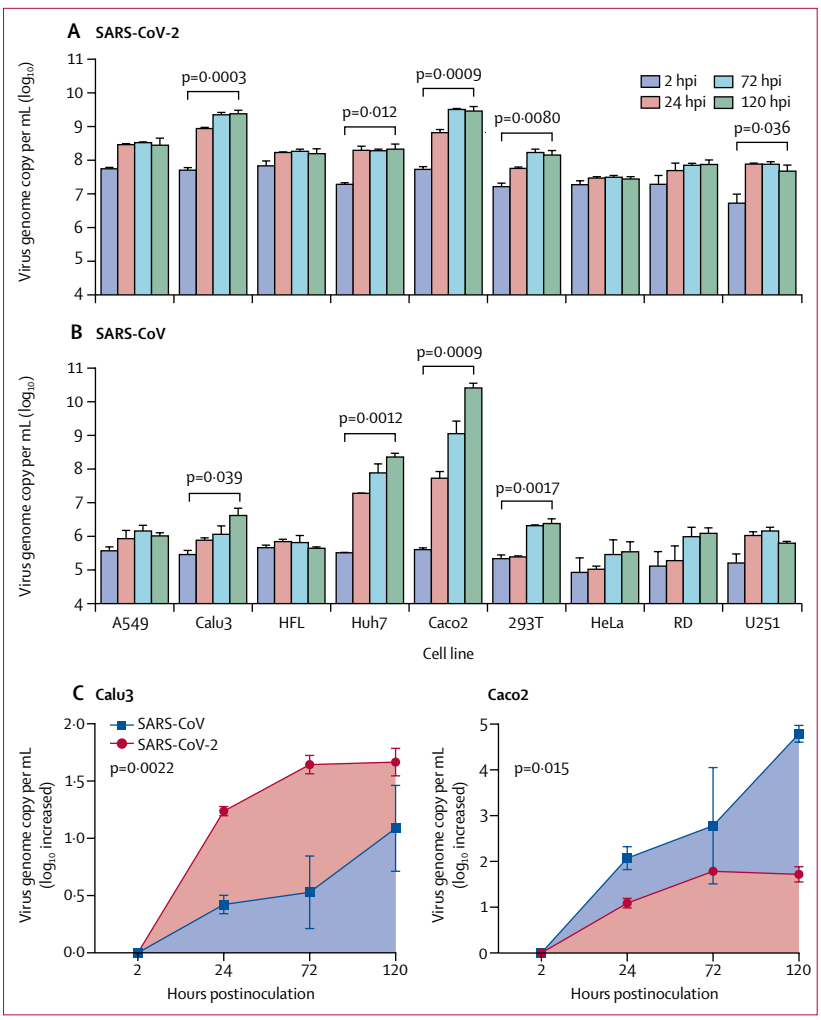

Figure 1: **Cell tropism profile of SARS-CoV-2 in human cells originating from different organ tissues**
Nine cell lines from different human tissues or organs were challenged with SARS-CoV-2 (A) or SARS-CoV (B) at 0·1 MOI. Viral supernatant samples were harvested at 2 hpi, 24 hpi, 72 hpi, and 120 hpi. Viral loads were ascertained with quantitative RT-PCR. For each cell type, the mean viral load at 120 hpi was compared with the mean baseline viral load at 2 hpi. (C) Area under the curve analysis of Calu3 (pulmonary) and Caco2 (intestinal) cells infected with SARS-CoV-2 and SARS-CoV. Bars (A, B) or datapoints (C) represent the mean (error bars show SD) of three independent experiments. Statistical significance was calculated with one-way ANOVA (A, B) or Student's *t* test (C). SARS-CoV-2=severe acute respiratory syndrome coronavirus 2. SARS-CoV=severe acute respiratory syndrome coronavirus. MOI=multiplicity of infection. hpi=hours postinoculation.

SARS-CoV at a multiplicity of infection (MOI) of 0·1 for 2 h at 37°C. Depending on the cell type, we maintained cells in minimum essential medium (Gibco, Waltham, MA, USA), Dulbecco's modified Eagle's medium (DMEM; Gibco), or DMEM/F12 (Gibco), according to suppliers' instructions. The cell lines we used are routinely tested for mycoplasma and are maintained mycoplasma-free.

RNA extraction and quantitative RT-PCR

We harvested supernatant samples from infected cells at 2 hpi, 24 hpi, 72 hpi, and 120 hpi for quantitative RT-PCR analysis of virus replication, as previously described.[16] Briefly, we lysed 100 µL of viral supernatant then extracted total RNA with QIAamp viral RNA mini kit (Qiagen, Hilden, Germany). We used real-time quantitative RT-PCR to quantify SARS-CoV-2 and SARS-CoV replication, using QuantiNova Probe RT-PCR kit (Qiagen) with a LightCycler 480 Real-Time PCR System (Roche, Basel, Switzerland). Each 20 µL reaction mixture contained 10 µL of 2×QuantiNova Probe RT-PCR Master Mix (Qiagen), 1·2 µL of RNase-free water, 0·2 µL of QuantiNova Probe RT-Mix (Qiagen), 1·6 µL each of 10 µmol/L forward and reverse primer, 0·4 µL of 10 µmol/L probe, and 5 µL of extracted RNA as template. We incubated the reactions at 45°C for 10 min for reverse transcription, 95°C for 5 min for denaturation, followed by 45 cycles of 95°C for 5 s and 55°C for 30 s. We detected and measured the signal in each cycle after the annealing step. The cycling profile ended with a cooling step at 40°C for 30 s. Primers and probe sequences were against the RNA-dependent RNA polymerase and helicase gene region of SARS-CoV-2 and SARS-CoV (panel).

Generation and titration of immune serum

To prepare antibodies against the nucleocapsid protein (NP) of SARS-CoV-2, we mixed 100 µg of purified SARS-CoV-2-NP recombinant protein with an equal volume of complete Freund's adjuvant (Sigma-Aldrich, St Louis, MO, USA) and injected the mixture subcutaneously into 4–6-week-old New Zealand white rabbits. We used incomplete Freund's adjuvant (Sigma-Aldrich) for three subsequent injections at 14-day intervals. We obtained serum samples after the third injection. For titration of the immune serum, we coated 96-well immunoplates (Nunc Immuno modules, Nunc, Denmark) with 100 µL per well (0·1 µg per well) of SARS-CoV-2-NP in 0·05 mol/L $NaHCO_3$ (pH 9·6) overnight at 4°C, followed by incubation with a blocking reagent. After blocking, we added to the wells 100 µL serial-diluted immunised rabbit SARS-CoV-2-NP or SARS-CoV-NP serum (starting from a dilution of 1/1000) and incubated the plates at 37°C for 1 h. After the plates were washed, we added horseradish peroxidase-labelled goat anti-rabbit antibody (Invitrogen, Carlsbad, CA, USA) at 100 µL per well, and we incubated the plates for 30 mins at 37°C. After incubation, we washed the wells then added 3,3',5,5'-tetramethylbenzidine solution (Invitrogen). After 10 min of reaction time, we stopped the reactions in the wells with 0·3 N sulphuric acid. We read the optical density at 450 nm with a plate reader (Perkin Elmer, Waltham, MA, USA).

Immunostaining and confocal microscopy

To detect antigen expression in SARS-CoV-2-infected cells, we used an in-house rabbit antiserum against SARS-CoV-2-NP. We labelled cell nuclei with the DAPI nucleic acid stain (ThermoFisher Scientific, Waltham, MA, USA). The secondary antibody was Alexa Fluor (ThermoFisher Scientific). Mounting was done with the Diamond Prolong Antifade mountant (ThermoFisher Scientific). We

acquired images with confocal microscopy using the Carl Zeiss LSM780 system (Zeiss, Oberkochen, Germany) with the 40×oil immersion objective, as previously described.[17]

Cell viability assays and imaging of cytopathic effect

To ascertain cell damage on SARS-CoV-2 and SARS-CoV infection, we quantified cell viability with the CellTiterGlo assay (Promega, Madison, WI, USA). We lysed cells together with culture supernatant at a ratio of 1:1 (volume) with the CellTiter-Glo reagent and incubated this mixture at room temperature for 10 min, then we measured the luminescence signal with the Vector X3 multilabel plate reader (Perkin Elmer). We obtained images of cellular cytopathic effect on SARS-CoV-2 and SARS-CoV infection at 72 hpi with a Nikon Ts2R-FL inverted microscope (Nikon, Tokyo, Japan).

Recombinant human ACE2 blocking assay

We preincubated SARS-CoV-2 or SARS-CoV with 80 µg/mL recombinant human angiotensin-converting enzyme (ACE) 2 (R&D Systems, Minneapolis, MN, USA) for 1 h. We added the mixture to VeroE6 cells for 30 min. Subsequently, we washed cells and incubated them with fresh medium for 4 h before cell lysates were harvested for quantitative RT-PCR analysis of virus genome copies.

Statistical analysis

We compared SARS-CoV-2 or SARS-CoV replication in different cell lines with one-way ANOVA. For the area under the curve (AUC) comparison between SARS-CoV-2 or SARS-CoV replication in Calu3 (pulmonary) and Caco2 (intestinal) cells, we used Student's *t* test. We analysed cell damage induced by SARS-CoV-2 or SARS-CoV with one-way ANOVA. All analyses were done with GraphPad Prism version 6 (GraphPad, San Diego, CA, USA). We judged differences statistically significant when p values were less than 0·05.

Role of the funding source

The funders had no role in study design, data collection, data analysis, data interpretation, or writing of the report. The corresponding author had full access to all data in the study and had final responsibility for the decision to submit for publication.

Results

Of nine human cell lines tested (table), five were susceptible to SARS-CoV-2 infection, as shown by significant virus replication over a period of 120 h (figure 1A). Among these susceptible cell lines, SARS-CoV-2 replication was most robust in Calu3 (pulmonary; p=0·0003) and Caco2 (intestinal; p=0·0009) cells, followed by Huh7 (hepatic; p=0·012) and 293T (renal; p=0·0080) cells. Furthermore, modest SARS-CoV-2 replication was detected in U251 (neuronal; p=0·036) cells. In general, the cellular tropism of SARS-CoV-2 was similar to that of SARS-CoV, which also showed significant virus replication in Calu3 (p=0·039), Caco2 (p=0·0009), Huh7 (p=0·0012), and 293T (p=0·0017) cells, but not in U251 cells (figure 1B). Although SARS-CoV showed higher replication capacity in Caco2 cells than in Calu3 cells (>3·5 log difference between Caco2 and Calu3 at 120 hpi; p=0·0098), SARS-CoV-2 replicated efficiently in both Caco2 and Calu3 cells (<0·1 log difference between Caco2 and Calu3 at 120 hpi; p=0·52). These findings were supported by the AUC analysis, which showed that the total virus production in Calu3 cells infected by SARS-CoV-2 was significantly higher than that of SARS-CoV (p=0·0022), but the total virus production in Caco2 cells infected by SARS-CoV was significantly higher than that of SARS-CoV-2 (p=0·015), over the 120 h period (figure 1C). The difference in SARS-CoV-2 and SARS-CoV replication in Calu3 and Caco2 cells was further validated by assays to ascertain the median tissue culture infectious dose (appendix p 3). Overall, despite SARS-CoV-2 and SARS-CoV sharing a similar profile of cellular tropism, the two viruses might differ in their capacity to infect or replicate in pulmonary, intestinal, and neuronal cells.

Of 16 non-human cell lines tested (table), six were susceptible to SARS-CoV-2 infection over a period of

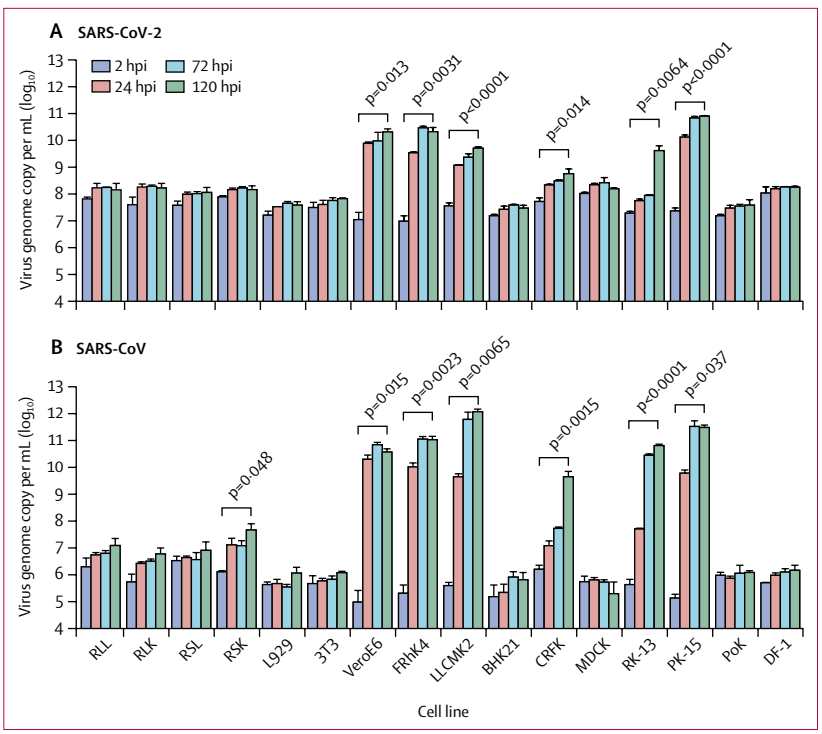

Figure 2: **Cell tropism profile of SARS-CoV-2 in non-human cells originating from different animal species**
16 non-human cell lines were challenged with SARS-CoV-2 (A) or SARS-CoV (B) at 0·1 MOI. Viral supernatant samples were harvested at 2 hpi, 24 hpi, 72 hpi, and 120 hpi. Viral loads were ascertained with quantitative RT-PCR. For each cell type, the mean viral load at 120 hpi was compared with the mean baseline viral load at 2 hpi. Bars represent the mean (error bars show SD) of three independent experiments. Statistical significance was calculated with one-way ANOVA. SARS-CoV-2=severe acute respiratory syndrome coronavirus 2. SARS-CoV=severe acute respiratory syndrome coronavirus. MOI=multiplicity of infection. hpi=hours postinoculation.

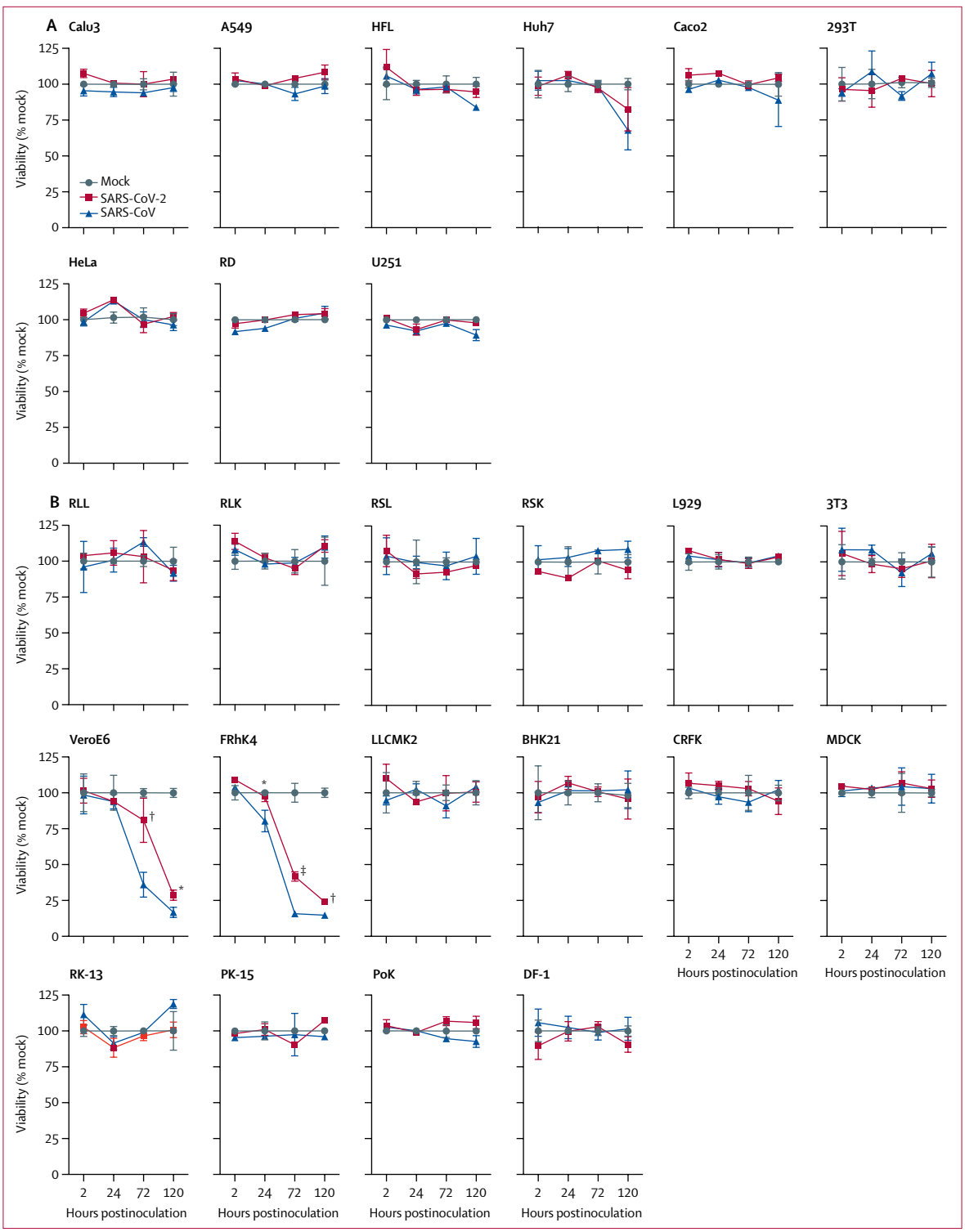

Figure 3: **Cell viability profile of SARS-CoV-2-inoculated and SARS-CoV-inoculated cells**
The cell viability of nine human cell lines (A) and 16 non-human cell lines (B) on SARS-CoV-2 or SARS-CoV infection at 0·1 MOI was quantified at 2 hpi, 24 hpi, 72 hpi, and 120 hpi. For VeroE6 and FRhK4 cells, the mean cell viability of SARS-CoV-2-inoculated cells at each timepoint was compared with that of SARS-CoV-inoculated cells. Datapoints represent the mean (error bars show SD) of three independent experiments. Statistical significance between groups was calculated with one-way ANOVA. SARS-CoV-2=severe acute respiratory syndrome coronavirus 2. SARS-CoV=severe acute respiratory syndrome coronavirus. MOI=multiplicity of infection. hpi=hours postinoculation. *p=0·013. †p=0·0044. ‡p=0·0008.

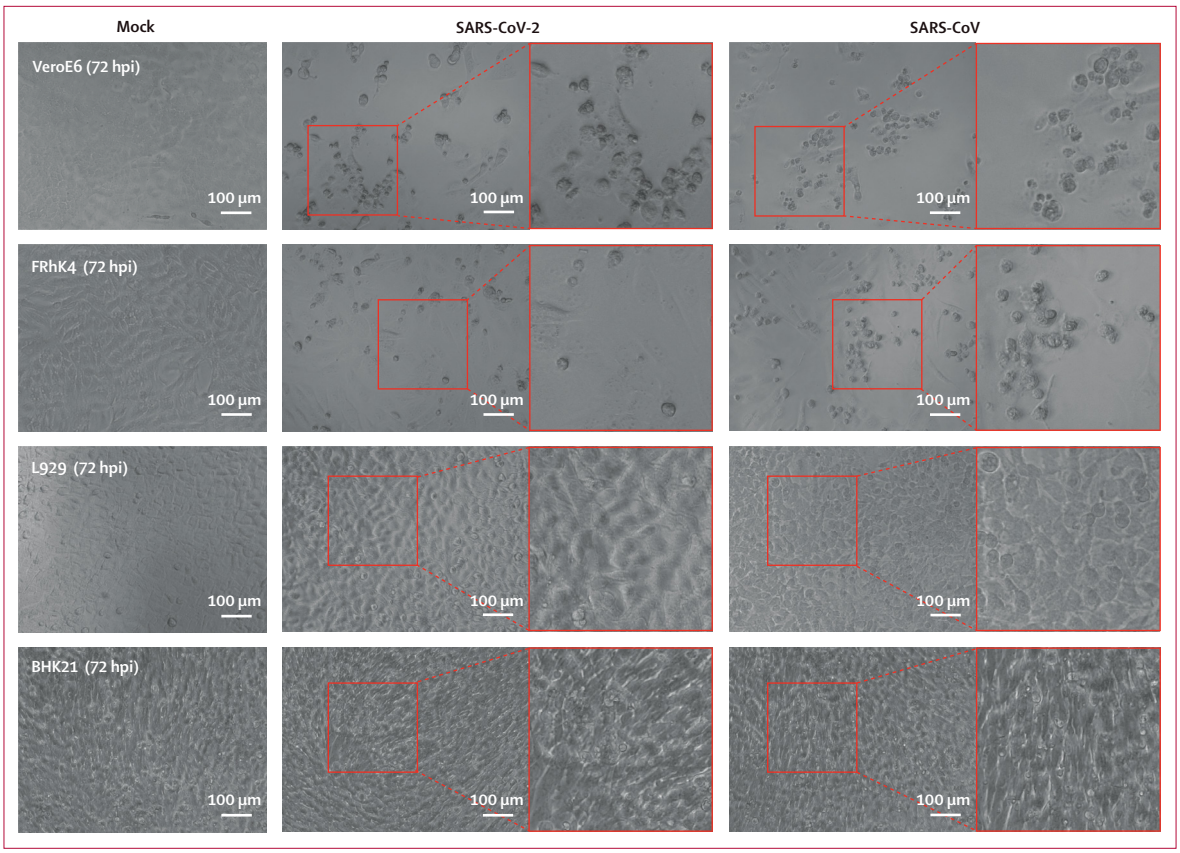

Figure 4: **Detection of SARS-CoV-2-induced cytopathic effects in representative cell types**
SARS-CoV-2-induced cytopathic effects were assessed in VeroE6 and FRhK4 cells. L929 and BHK21 cells were included as negative controls. Cells were infected with SARS-CoV-2 or SARS-CoV at 0·1 MOI. At 72 hpi, typical cytopathic effects were seen, including cell rounding, detachment, degeneration, and syncytium formation. Boxed area is shown adjacent to each image. Cells were imaged with a Nikon Ts2R-FL inverted microscope. Bars represent 100 µm. SARS-CoV-2=severe acute respiratory syndrome coronavirus 2. SARS-CoV=severe acute respiratory syndrome coronavirus. MOI=multiplicity of infection. hpi=hours postinoculation.

120 h, including cells originating from non-human primates (VeroE6 [p=0·013], FRhK4 [p=0·0031], and LLCMK2 [p<0·0001]), cat (CRFK [p=0·014]), rabbit (RK-13 [p=0·0064]), and pig (PK-15 [p<0·0001]; figure 2A). SARS-CoV-2 replicated most robustly in non-human primate cells and pig cells, as shown by a 3 log or greater increase in mean viral load over a period of 120 h in VeroE6, FRhK4, and PK-15 cells. Similar to the human cell tropism profile, the cellular tropism of SARS-CoV-2 in non-human cells largely matched that of SARS-CoV, which was also capable of infecting and replicating in non-human primate, cat, rabbit, and pig cells (figure 2B). Importantly, SARS-CoV, but not SARS-CoV-2, could replicate in *Rhinolophus sinicus* primary bat kidney cells (RSK; p=0·048). With the recombinant human ACE2 protein blocking assay, we confirmed that, similar to SARS-CoV, infection of SARS-CoV-2 was dependent on ACE2 (appendix p 4).

In addition to cellular tropism and replication kinetics profiles, cell damage induced by SARS-CoV-2 was also assessed in nine human (figure 3A) and 16 non-human (figure 3B) cell lines. Among the 11 cell lines that supported SARS-CoV-2 replication (Calu3, Huh7, Caco2, 293T, U251, VeroE6, FRhK4, LLCMK2, CRFK, RK-13, and PK-15), SARS-CoV-2 only induced substantial cell damage in VeroE6 cells (28·7% viability at 120 hpi; p<0·0001) and FRhK4 cells (24·0% viability at 120 hpi; p<0·0001). Typical cytopathic effects in VeroE6 and FRhK4 cells included cell rounding, detachment, degeneration, and syncytium formation (figure 4).

Despite robust SARS-CoV-2 replication in Calu3 and Caco2 cells, substantial cell death was not detected up to 120 hpi (at 120 hpi, Calu3 viability was 103% and Caco2 viability was 104%). To understand if SARS-CoV-2 would induce cell death in cells that supported efficient virus replication at a delayed timepoint, cell viability of SARS-CoV-2-infected Calu3, Caco2, LLCMK2, PK-15, and RK-13 cells was assessed at 7 days postinfection; cell death was not detected in these cell types (appendix p 5).

Although SARS-CoV-2 and SARS-CoV were inoculated with the same MOI, SARS-CoV-2 induced less cell damage than did SARS-CoV (figure 3). This observation was supported by the significantly higher percentage of cell viability in VeroE6 and FRhK4 cells infected by SARS-CoV-2 than in those infected by SARS-CoV, at multiple timepoints. The AUC analysis also showed a

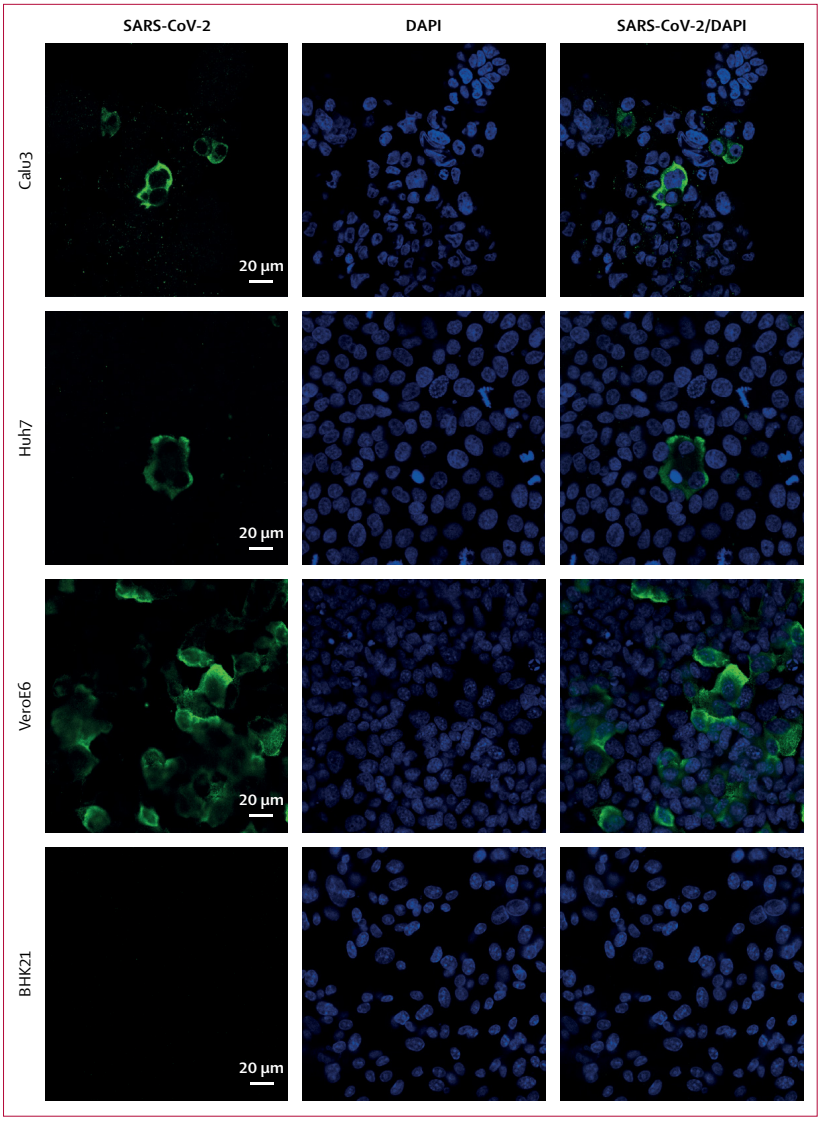

Figure 5: **Antigen expression of SARS-CoV-2**
Antigen expression of SARS-CoV-2 was assessed in several representative cell types, including Calu3, Huh7, and VeroE6 cells; BHK21 cells were included as a negative control. Cells were infected with SARS-CoV-2 at 0·1 MOI. At 16 hpi, cells were fixed in 4% paraformaldehyde and immunolabelled with an in-house rabbit anti-SARS-CoV-2-NP immune serum. Confocal images were acquired with a Zeiss LSM780 system. Bars represent 20 μm. SARS-CoV-2=severe acute respiratory syndrome coronavirus 2. DAPI=nucleic acid stain. MOI=multiplicity of infection. hpi=hours postinoculation. SARS-CoV-2-NP=SARS-CoV-2 nucleocapsid protein.

significantly higher amount of viable cells on SARS-CoV-2 infection by comparison with SARS-CoV infection in both VeroE6 cells (p=0·016) and FRhK4 cells (p=0·0004) over the 120 h period (appendix p 6).

In parallel with the viral replication assays, SARS-CoV-2 antigen expression was detected in several representative cell types using antiserum against the SARS-CoV-2-NP antibody (appendix p 7). By immunostaining and confocal microscopy, SARS-CoV-2-NP could be abundantly detected at as early as 16 hpi. SARS-CoV-2-NP appeared diffusely distributed across the cytoplasm of the infected cells (appendix p 8). The abundance of antigen expression corresponded with viral replication kinetics (appendix p 9). Abundant SARS-CoV-2-NP expression was detected in cell lines that supported SARS-CoV-2 replication, including VeroE6, Calu3, and Huh7 cells. By contrast, viral antigen expression was not detected from non-susceptible BHK21 cells inoculated with SARS-CoV-2 (figure 5).

Discussion

In the past 3 months, most publications on COVID-19 have been observational studies in clinical cohorts, epidemiological investigations and forecasts, and in-silico genomic and structural analyses. Many basic virological questions of SARS-CoV-2 remain unanswered. In this study, we systematically compared the differential cell tropism, viral replication kinetics, and cell damage profiles of SARS-CoV-2 and SARS-CoV. Our data show biological characteristics of SARS-CoV-2 that might provide insights into understanding this virus's unique clinical manifestations and transmissibility and rationalising laboratory diagnostics.

As expected from use of human ACE2 as an entry receptor, SARS-CoV-2 and SARS-CoV showed significant replication in Calu3 (pulmonary) cells, which corresponds with the abilities of these coronaviruses to cause lower respiratory tract infection. By contrast, HCoV-229E, which primarily causes self-limiting upper respiratory tract infection, does not replicate efficiently in Calu3 cells.[20] SARS-CoV-2 replicated to comparable levels in both Calu3 and Caco2 (intestinal) cells, whereas SARS-CoV replicated significantly more efficiently in Caco2 than in Calu3 cells, with the same MOI. This finding supports the higher incidence of diarrhoea in patients with SARS than in COVID-19 patients. Among 337 patients with COVID-19 reported in four large clinical cohorts,[6–9] only 20 (6%) developed diarrhoea. By contrast, diarrhoea was the most common extrapulmonary clinical manifestation of SARS and was reported in up to 130 (20%) of 647 SARS patients.[5] Clinical deterioration of SARS commonly occurred 1 week after symptom onset and was typically accompanied by non-inflammatory watery diarrhoea.[21] The mean viral load in stool specimens from SARS patients was 1·2 $\log_{10}$ copies per mL higher than that in nasopharyngeal aspirate specimens at days 10–15 after symptom onset.[22]

Among other non-pulmonary cell lines, SARS-CoV-2 and SARS-CoV both showed significant replication in Huh7 (hepatic) and 293T (renal) cells. Up to 43% of patients with COVID-19 and 44% of SARS patients developed hepatic dysfunction.[5,8] Patients with COVID-19 needing intensive care had significantly higher amounts of hepatic aminotransferases than did those not needing intensive care.[6] In terms of renal manifestations, 3–7% of patients with COVID-19 developed acute kidney injury or needed renal replacement therapy.[6,8,9] Similarly, 7% of SARS patients developed acute renal impairment, which was associated with a significantly higher mortality rate than in those without acute renal impairment (91·7% *vs*

8·8%; p<0·0001).[23] The prognostic value of hepatic and renal dysfunction in patients with COVID-19 should be further investigated.

Our data show modest replication of SARS-CoV-2, but not SARS-CoV, in U251 (neuronal) cells. This finding might correlate with the observation that up to 9% of patients with COVID-19 develop confusion or dizziness, and some are reported to have anosmia and ageusia,[6,8,24] whereas these neurological manifestations were rarely reported in SARS patients.[5] The potential for SARS-CoV-2 to directly infect the CNS needs closer scrutiny, because another betacoronavirus (HCoV-OC43) has been associated with fatal encephalitis in an 11-month-old boy with severe combined immunodeficiency.[25]

Our data also provide new insights into the apparently high transmissibility of SARS-CoV-2. In the AUC analysis, SARS-CoV-2 showed more efficient replication in Calu3 cells than did SARS-CoV. Both SARS-CoV-2 and SARS-CoV can use human ACE2 as a cell entry receptor.[3] However, the spike protein S1 subunits of the two viruses share only approximately 70% amino acid identity.[26] Significant amino acid differences between SARS-CoV-2 and SARS-CoV are located in the ectodomain of the spike protein, which is important for receptor binding.[26] Findings of a study showed that the binding affinity between the SARS-CoV-2 spike ectodomain and human ACE2 was approximately 10–20-fold higher than the binding affinity between the SARS-CoV spike ectodomain and human ACE2.[27] This higher receptor-binding capacity might facilitate virus entry into pulmonary cells and lead to more efficient person-to-person transmission through direct or indirect contact with respiratory droplets from patients with COVID-19.

Although SARS-CoV-2 and SARS-CoV showed similar tropism in 16 non-human cell lines derived from various animal species, SARS-CoV, but not SARS-CoV-2, showed significant replication in RSK cells. We and others have previously identified *R sinicus* as the likely natural animal reservoir of SARS-like coronavirus.[28,29] SARS-CoV-2 has been postulated to originate from *R sinicus* bats, because the virus is phylogenetically most closely related to coronaviruses found in these bats.[26] Our findings raise the possibility that SARS-CoV-2 has already adapted well to humans and, thus, the virus is no longer able to propagate well in *R sinicus* bat cells, providing a possible explanation for the efficient person-to-person transmission of COVID-19.

Our cell culture model data are useful for optimising laboratory methods for studying COVID-19. First, we showed that SARS-CoV-2 replicated efficiently in non-human primate (VeroE6, FRhK4, LLCMK2), cat (CRFK), rabbit (RK-13), and pig (PK-15) cells. Non-human primates (including Rhesus macaques, cynomolgus macaques, African green monkeys, and common marmosets) were susceptible to infection with SARS-CoV, MERS-CoV, or both viruses.[30] SARS-CoV-infected domestic cats developed asymptomatic infection with virus shedding from their pharynx from days 2 to 14 post infection.[31] Similarly, MERS-CoV-infected rabbits and domestic pigs also developed asymptomatic virus shedding from their respiratory tract.[32,33] The susceptibility of mice transgenic for human ACE2 to SARS-CoV-2 infection should be assessed so animal models can be developed that could recapitulate the different disease severities of COVID-19 in humans (ranging from asymptomatic to fatal infection). Second, our data show that the abundance of SARS-CoV-2 antigen expression correlated with viral replication kinetics. Although immunofluorescent antigen tests generally have lower sensitivity than do RT-PCR assays, this non-labour-intensive diagnostic could be considered as a screening test in laboratories without the resources and expertise for RT-PCR assays for COVID-19. Finally, our data show that among the 25 cell lines assessed, cytopathic effects were only seen in VeroE6 and FRhK4 cells after SARS-CoV-2 inoculation for up to 120 hpi. These findings are important for optimisation of antiviral assays based on cell protection assessment, because cell lines without obvious cytopathic effects might lead to overestimation of cell viability and drug efficacy.

Our study had several limitations. First, cell line tropism might not fully represent how SARS-CoV-2 replicates and affects human organs in the physiological state. Thus, our cell line susceptibility results and the clinical manifestations of patients with COVID-19 might not completely accord. It is essential to further characterise virus–host interactions in more physiological models, such as ex-vivo human organ tissue and human organoids from patients of different ages, sexes, and with underlying diseases. Nevertheless, findings in cell line susceptibility studies of MERS-CoV were highly corroborative with those seen in patients with MERS.[13] Second, for all our experiments, we used one viral isolate that was highly homologous to other reported SARS-CoV-2 isolates. Isolates with additional amino acid mutations, particularly involving the receptor binding domain, should be studied to identify viral factors that might affect virus entry to host cells and virus replication kinetics. Finally, the viral kinetics of SARS-CoV-2 in other human cell lines (eg, cardiomyocytes) and animal cell lines should be assessed to investigate virus-induced damage in cardiac cells and potential animal reservoirs.

Contributors

HC, JF-WC, and K-YY contributed to study design, data collection, data analysis, data interpretation, and writing of the report. TT-TY, HS, SY, YW, BH, CC-YY, JO-LT, XH, YC, DY, YH, KK-HC, XZ, AY-FF, H-WT, J-PC, W-MC, JDI, AW-HC, JZ, DCL, K-HK, KK-WT, OT-YT, and K-HC contributed to the experiments, data collection, data analysis, and data interpretation. All authors reviewed and approved the final version of the report.

Declaration of interests

We declare no competing interests.

Acknowledgments

This study was partly supported by donations from May Tam Mak Mei Yin, the Shaw Foundation Hong Kong, Richard Yu and Carol Yu, Michael Seak-Kan Tong, Respiratory Viral Research Foundation, Hui Ming, Hui Hoy and Chow Sin Lan Charity Fund, Chan Yin Chuen

Memorial Charitable Foundation, Marina Man-Wai Lee, the Hong Kong Hainan Commercial Association South China Microbiology Research Fund, the Jessie & George Ho Charitable Foundation, and Perfect Shape Medical; and by funding from the Consultancy Service for Enhancing Laboratory Surveillance of Emerging Infectious Diseases and Research Capability on Antimicrobial Resistance for the Department of Health of the Hong Kong Special Administrative Region Government; the Theme-Based Research Scheme (T11/707/15) of the Research Grants Council; Hong Kong Special Administrative Region; Sanming Project of Medicine in Shenzhen, China (no SZSM201911014); and the High Level-Hospital Program, Health Commission of Guangdong Province, China.

References

1 Chan JF, Lau SK, To KK, Cheng VC, Woo PC, Yuen KY. Middle East respiratory syndrome coronavirus: another zoonotic betacoronavirus causing SARS-like disease. *Clin Microbiol Rev* 2015; **28:** 465–522.

2 Zhu N, Zhang D, Wang W, et al. A novel coronavirus from patients with pneumonia in China, 2019. *N Engl J Med* 2020; **382:** 727–33.

3 Zhou P, Yang XL, Wang XG, et al. A pneumonia outbreak associated with a new coronavirus of probable bat origin. *Nature* 2020; **579:** 270–73.

4 Chan JF-W, Yuan S, Kok K-H, et al. A familial cluster of pneumonia associated with the 2019 novel coronavirus indicating person-to-person transmission: a study of a family cluster. *Lancet* 2020; **395:** 514–23.

5 Cheng VC, Lau SK, Woo PC, Yuen KY. Severe acute respiratory syndrome coronavirus as an agent of emerging and reemerging infection. *Clin Microbiol Rev* 2007; **20:** 660–94.

6 Wang D, Hu B, Hu C, et al. Clinical characteristics of 138 hospitalized patients with 2019 novel coronavirus-infected pneumonia in Wuhan, China. *JAMA* 2020; **323:** 1061–69.

7 Xu XW, Wu XX, Jiang XG, et al. Clinical findings in a group of patients infected with the 2019 novel coronavirus (SARS-Cov-2) outside of Wuhan, China: retrospective case series. *BMJ* 2020; **368:** m606.

8 Chen N, Zhou M, Dong X, et al. Epidemiological and clinical characteristics of 99 cases of 2019 novel coronavirus pneumonia in Wuhan, China: a descriptive study. *Lancet* 2020; **395:** 507–13.

9 Huang C, Wang Y, Li X, et al. Clinical features of patients infected with 2019 novel coronavirus in Wuhan, China. *Lancet* 2020; **395:** 497–506.

10 Bauch CT, Lloyd-Smith JO, Coffee MP, Galvani AP. Dynamically modeling SARS and other newly emerging respiratory illnesses: past, present, and future. *Epidemiology* 2005; **16:** 791–801.

11 Liu Y, Gayle AA, Wilder-Smith A, Rocklov J. The reproductive number of COVID-19 is higher compared to SARS coronavirus. *J Travel Med* 2020; **27:** taaa021.

12 Shen M, Peng Z, Xiao Y, Zhang L. Modelling the epidemic trend of the 2019 novel coronavirus outbreak in China. Jan 25, 2020. https://www.biorxiv.org/content/10.1101/2020.01.23.916726v1 (accessed March 26, 2020) (preprint).

13 Chan JF, Chan KH, Choi GK, et al. Differential cell line susceptibility to the emerging novel human betacoronavirus 2c EMC/2012: implications for disease pathogenesis and clinical manifestation. *J Infect Dis* 2013; **207:** 1743–52.

14 Chan JF, Yip CC, Tsang JO, et al. Differential cell line susceptibility to the emerging Zika virus: implications for disease pathogenesis, non-vector-borne human transmission and animal reservoirs. *Emerg Microbes Infect* 2016; **5:** e93.

15 Kaye M. SARS-associated coronavirus replication in cell lines. *Emerg Infect Dis* 2006; **12:** 128–33.

16 Chan JF, Yip CC, To KK, et al. Improved molecular diagnosis of COVID-19 by the novel, highly sensitive and specific COVID-19-RdRp/Hel real-time reverse transcription-polymerase chain reaction assay validated in vitro and with clinical specimens. *J Clin Microbiol* 2020; published online March 4. DOI:10.1128/JCM.00310-20.

17 Chu H, Chan CM, Zhang X, et al. Middle East respiratory syndrome coronavirus and bat coronavirus HKU9 both can utilize GRP78 for attachment onto host cells. *J Biol Chem* 2018; **293:** 11709–26.

18 Edgar RC. MUSCLE: multiple sequence alignment with high accuracy and high throughput. *Nucleic Acids Res* 2004; **32:** 1792–97.

19 Kumar S, Stecher G, Li M, et al. MEGA X: molecular evolutionary genetics analysis across computing platforms. *Mol Biol Evol* 2018; **35:** 1547–49.

20 Lau SK, Lau CC, Chan KH, et al. Delayed induction of proinflammatory cytokines and suppression of innate antiviral response by the novel Middle East respiratory syndrome coronavirus: implications for pathogenesis and treatment. *J Gen Virol* 2013; **94:** 2679–90.

21 Cheng VC, Hung IF, Tang BS, et al. Viral replication in the nasopharynx is associated with diarrhea in patients with severe acute respiratory syndrome. *Clin Infect Dis* 2004; **38:** 467–75.

22 Hung IF, Cheng VC, Wu AK, et al. Viral loads in clinical specimens and SARS manifestations. *Emerg Infect Dis* 2004; **10:** 1550–57.

23 Chu KH, Tsang WK, Tang CS, et al. Acute renal impairment in coronavirus-associated severe acute respiratory syndrome. *Kidney Int* 2005; **67:** 698–705.

24 Vaira LA, Salzano G, Deiana G, De Riu G. Anosmia and ageusia: common findings in COVID-19 patients. *Laryngoscope* 2020; published online April 1. DOI:10.1002/lary.28692.

25 Morfopoulou S, Brown JR, Davies EG, et al. Human coronavirus OC43 associated with fatal encephalitis. *N Engl J Med* 2016; **375:** 497–98.

26 Chan JF, Kok KH, Zhu Z, et al. Genomic characterization of the 2019 novel human-pathogenic coronavirus isolated from a patient with atypical pneumonia after visiting Wuhan. *Emerg Microbes Infect* 2020; **9:** 221–36.

27 Wrapp D, Wang N, Corbett KS, et al. Cryo-EM structure of the 2019-nCoV spike in the prefusion conformation. *Science* 2020; **367:** 1260–63.

28 Ge XY, Li JL, Yang XL, et al. Isolation and characterization of a bat SARS-like coronavirus that uses the ACE2 receptor. *Nature* 2013; **503:** 535–38.

29 Lau SK, Woo PC, Li KS, et al. Severe acute respiratory syndrome coronavirus-like virus in Chinese horseshoe bats. *Proc Natl Acad Sci USA* 2005; **102:** 14040–45.

30 Gretebeck LM, Subbarao K. Animal models for SARS and MERS coronaviruses. *Curr Opin Virol* 2015; **13:** 123–29.

31 Martina BE, Haagmans BL, Kuiken T, et al. Virology: SARS virus infection of cats and ferrets. *Nature* 2003; **425:** 915.

32 Haagmans BL, van den Brand JM, Provacia LB, et al. Asymptomatic Middle East respiratory syndrome coronavirus infection in rabbits. *J Virol* 2015; **89:** 6131–35.

33 de Wit E, Feldmann F, Horne E, et al. Domestic pig unlikely reservoir for MERS-CoV. *Emerg Infect Dis* 2017; **23:** 985–88.